Article

Cell Reports

Necroptosis Promotes *Staphylococcus aureus* Clearance by Inhibiting Excessive Inflammatory Signaling

Graphical Abstract

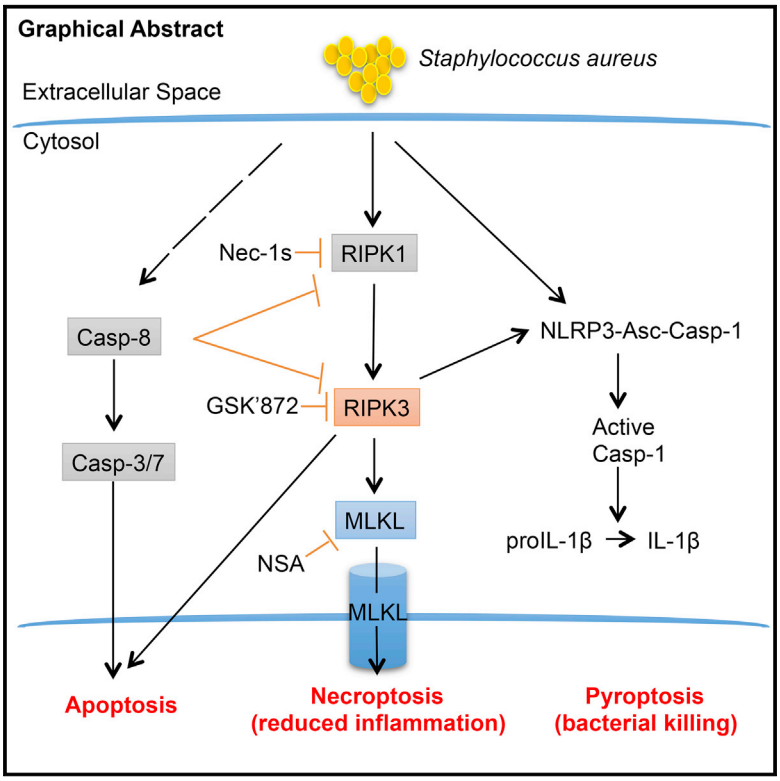

Highlights

- *S. aureus* activates RIPK1/RIPK3/MLKL-mediated necroptosis
- *Mlkl*−/− mice have increased inflammation and infection
- Necroptosis regulates inflammation in skin and systemic infection

Authors

Kipyegon Kitur, Sarah Wachtel, Armand Brown, ..., Susan Bueno, Dane Parker, Alice Prince

Correspondence

asp7@columbia.edu

In Brief

Kitur et al. find that *S. aureus* activates necroptosis in models of cutaneous and systemic infection. This mechanism of cell death serves to limit excessive inflammatory responses, especially IL-1β production, and improves bacterial clearance.

Kitur et al., 2016, Cell Reports *16*, 2219–2230
August 23, 2016
http://dx.doi.org/10.1016/j.celrep.2016.07.039

Cell Reports
Article

Necroptosis Promotes *Staphylococcus aureus* Clearance by Inhibiting Excessive Inflammatory Signaling

Kipyegon Kitur,[1] Sarah Wachtel,[2] Armand Brown,[2] Matthew Wickersham,[2] Franklin Paulino,[2] Hernán F. Peñaloza,[3] Grace Soong,[2] Susan Bueno,[3] Dane Parker,[2] and Alice Prince[1,2,*]
[1]Department of Pharmacology, Columbia University, New York, NY 10032, USA
[2]Department of Pediatrics, College of Physicians and Surgeons, Columbia University, New York, NY 10032, USA
[3]Millennium Institute on Immunology and Immunotherapy, Departamento de Genética Molecular y Microbiología, Facultad de Ciencias Biológicas, Pontificia Universidad Católica de Chile, Santiago 8331150, Chile
*Correspondence: asp7@columbia.edu
http://dx.doi.org/10.1016/j.celrep.2016.07.039

SUMMARY

***Staphylococcus aureus* triggers inflammation through inflammasome activation and recruitment of neutrophils, responses that are critical for pathogen clearance but are associated with substantial tissue damage. We postulated that necroptosis, cell death mediated by the RIPK1/RIPK3/MLKL pathway, would function to limit pathological inflammation. In models of skin infection or sepsis, *Mlkl*−/− mice had high bacterial loads, an inability to limit interleukin-1b (IL-1b) production, and excessive inflammation. Similarly, mice treated with RIPK1 or RIPK3 inhibitors had increased bacterial loads in a model of sepsis. *Ripk3*−/− mice exhibited increased staphylococcal clearance and decreased inflammation in skin and systemic infection, due to direct effects of RIPK3 on IL-1b activation and apoptosis. In contrast to *Casp1/4*−/− mice with defective *S. aureus* killing, the poor outcomes of *Mlkl*−/− mice could not be attributed to impaired phagocytic function. We conclude that necroptotic cell death limits the pathological inflammation induced by *S. aureus*.**

INTRODUCTION

Staphylococcus aureus causes pyogenic infections characterized by a robust inflammatory response both locally and systemically. This inflammation must be regulated to prevent host tissue damage. Multiple redundant proinflammatory signaling cascades are activated by *S. aureus* through pathogen-associated molecular patterns and toxins. Several *S. aureus* toxins activate the NLRP3 inflammasome and caspase-1 to generate interleukin-1β (IL-1β), IL-18, and pyroptosis, a highly proinflammatory mechanism of cell death (Craven et al., 2009; Muñoz-Planillo et al., 2009). Pyroptosis, along with the generation of reactive oxygen species (ROS) and the proteolytic activity of phagocytes, contributes to eradication of endocytosed pathogens (Miao et al., 2010; Sokolovska et al., 2013).

The balance between sufficient proinflammatory signaling to clear infection and the potentially lethal consequences of inflammasome activation has been extensively studied in the context of tumor necrosis factor (TNF)- and lipopolysaccharide (LPS)-induced mortality (Aziz et al., 2014; Duprez et al., 2011; Lawlor et al., 2015). Systemic effects of IL-1β and IL-18 are major factors in sepsis- and endotoxemia-associated mortality (Vanden Berghe et al., 2014a). Cell death through pyroptosis can also contribute to the control of infection, through release of endocytosed pathogens that are more efficiently killed by neutrophils (Miao et al., 2010).

Like immune cells, keratinocytes undergo caspase-1-mediated pyroptosis and IL-1β production in response to *S. aureus*, contributing to the eradication of skin infection (Soong et al., 2012, 2015). Keratinocytes follow a highly regulated pattern of proliferation, maturation, cornification, and cell death through several mechanisms, including apoptosis and necroptosis (Nestle et al., 2009; Vanden Berghe et al., 2014b). *S. aureus* through its pore-forming toxins induces necroptosis in immune cells (González-Juarbe et al., 2015; Kitur et al., 2015). Necroptosis results from oligomerization of MLKL (Murphy et al., 2013), which is initiated by RIPK3-dependent phosphorylation (Cai et al., 2014; Sun et al., 2012) and RIPK1 (Linkermann and Green, 2014). MLKL then forms a pore that leaks intracellular contents, with a resulting inflammatory response (Kaczmarek et al., 2013). Like caspase-1-mediated pyroptosis, necroptosis also results in the release of intracellular contents promoting inflammation. Necroptosis and pyroptosis share multiple effectors, with some of these components, including caspase-8, RIPK1, and RIPK3, contributing to the processing and activation of IL-1β (Kaczmarek et al., 2013; Moriwaki et al., 2015; Pasparakis and Vandenabeele, 2015). Thus, both pyroptosis and necroptosis generate substantial inflammation. RIPK1/RIPK3/MLKL signaling can be activated by Toll-like receptors (TLRs) and TNF receptor (TNFR)- and interferon alpha/beta receptor (IFNAR)-mediated responses, indicating the close association between necroptosis and pathogen recognition (Chan et al., 2015). However, the consequences of necroptosis are not necessarily proinflammatory. Necroptosis leads to the elimination of cells that produce cytokines and inflammatory products and the release of bacteria to be cleared by neutrophils, leading

to an overall decrease in inflammation (Kearney et al., 2015; Stephenson et al., 2016).

Exactly how necroptosis and pyroptosis function in host defense from *S. aureus* infection is unclear, given that both signaling pathways appear to have redundant effects, stimulating inflammatory signaling as well as cell death (Kang et al., 2013, 2015).

The successful control of *S. aureus* infection has been suggested to require two major host responses: first, the rapid suppression of *S. aureus* replication and, second, the rapid regulation of the hyper-inflammatory response that ensues (Powers et al., 2015; Stephenson et al., 2016). We postulated that pyroptosis initiates clearance of staphylococci and that necroptosis serves to eliminate cells that cause excessive inflammation. Using models of skin infection and sepsis, we delineate how these signaling pathways contribute to both of these components of successful host defense.

RESULTS

MLKL Contributes to the Clearance of *S. aureus* from Infected Skin

Murine models of skin infection provide the opportunity to monitor both inflammation and bacterial killing in an in vivo setting (Miller et al., 2006). To determine the role of necroptosis during skin infection, we compared the responses of *Mlkl*$^{-/-}$ mice, which are unable to undergo necroptosis (Murphy et al., 2013), with wild-type (WT) mice after a subcutaneous inoculation of USA300 *S. aureus* (Figure 1). In comparison to WT mice, there were significantly higher bacterial counts and more tissue damage in the *Mlkl*$^{-/-}$ mice (Figures 1A–1C). We confirmed that *S. aureus* infection activates necroptosis by documenting phosphorylated MLKL in infected human keratinocytes (Figure S1) and demonstrating that *S. aureus*-induced cytotoxicity was decreased significantly by inhibitors of MLKL (NSA) in human keratinocytes and primary cultures (Figures 1D and 1E) and by small interfering RNA (siRNA) knockdown of MLKL (Figures 1F and 1G) in keratinocytes. Thus, the ability of host cells to undergo necroptosis contributed to pathogen clearance.

We next determined whether excessive inflammation was contributing to the defective bacterial clearance exhibited by the *Mlkl*$^{-/-}$ mice. We compared the ability of these *Mlkl*$^{-/-}$ mice to activate proinflammatory cytokine production and to recruit the immune cells necessary to clear *S. aureus* infection. No differences between the WT, *Mlkl*$^{-/-}$ mice were observed after 1 day of infection either in the clearance of *S. aureus* or recruitment of immune cells (Figures S2A and S2B). However, by day 5, *Mlkl*$^{-/-}$ mice had significantly more neutrophils, macrophages, and $\gamma\delta$ T cells recruited than WT mice at the site of infection (Figures 1H–1J; Table S1). As early as 1 day post-infection, *Mlkl*$^{-/-}$ mice had increased T cell cytokine expression (IP-10/CXCL10, Rantes, and MIG; Figure S2C; Table S2), cytokines that mediate inflammatory damage in the skin (McLoughlin et al., 2006). Consistent with the heightened immune cell recruitment, by day 5, *Mlkl*$^{-/-}$ mice had significantly increased proinflammatory cytokines (IL-6, TNF, IL-1β, KC, and MIP1α; Figure 1K; Table S1).

The histopathological responses to infection also were different. *Mlkl*$^{-/-}$ mice exhibited increased necrosis and adiposity, a marker of inflammation (Rajala and Scherer, 2003; Schäffler and Schölmerich, 2010), in comparison to WT infected controls (Figure 1L). *Mlkl*$^{-/-}$ mice had hyperkeratosis and more immune cell infiltration as compared with the WT mice (Figure 1L). As increased IL-1β was observed in *Mlkl*$^{-/-}$ infections, tissue lysates were screened for the presence of active caspase-1 (Figure 1M). Substantially more caspase-1 p20 was found at both baseline and following infection in *Mlkl*$^{-/-}$ than in WT mice. The *Mlkl*$^{-/-}$ mice displayed increased caspase-1 activity; increased generation of proinflammatory cytokines, including IL-1β; and more neutrophils but were nonetheless unable to clear *S. aureus* as efficiently as the WT mice. Together, these results suggest that necroptosis participates in the regulation of excessive inflammation that causes tissue damage during *S. aureus* skin infection.

Lack of Caspases-1/4 Is Detrimental in *S. aureus* Skin Infection

We wanted to understand whether caspase-1 activation is beneficial during *S. aureus* skin infection. Production of IL-1β, which is processed by caspase-1, is critical for clearance of *S. aureus* from skin (Miller et al., 2006; Sokolovska et al., 2013; Soong et al., 2012). The contribution of the inflammasome to bacterial clearance was tested in *Casp1/4*$^{-/-}$ mice infected with *S. aureus* (Figure 2). The *Casp1/4*$^{-/-}$ knockout mice exhibited significantly decreased bacterial clearance and increased lesion sizes at 5 days after infection (Figures 2A–2C). Similar to *Mlkl*$^{-/-}$ mice, *Casp1/4*$^{-/-}$ mice had increased numbers of neutrophils and $\gamma\delta$ T cells, but not macrophages, at the site of infection (Figures 2D–2F). Unlike *Mlkl*$^{-/-}$ mice, which exhibited an increase in many proinflammatory cytokines, *Casp1/4*$^{-/-}$ mice had increased KC only and slightly, but not significantly, less IL-1β post-infection (Figure 2G; Table S3). Thus, caspase-1/4 activity is necessary for *S. aureus* clearance and contributes substantially to the generation of IL-1β.

Pharmacological Inhibition of RIPK1 Impairs Clearance and Increases Inflammation

To verify participation of necroptosis in staphylococcal clearance, we used a pharmacological inhibitor of the RIPK1 kinase activity necrostatin-1 s (Nec-1 s) (Degterev et al., 2008; Takahashi et al., 2012), which also obviates unanticipated effects of the germline mutation in the *Mlkl*$^{-/-}$ mice. After documenting that Nec-1 s blocked *S. aureus*-induced keratinocyte cell death in vitro (Figure 3A), we treated WT mice with Nec-1 s and monitored their response to *S. aureus* skin infection (Figures 3B–3D). Similar to the *Mlkl*$^{-/-}$ mice, the Nec-1-s-treated mice had significantly larger skin lesions, greater numbers of *S. aureus* recovered, and greater recruitment of inflammatory cells (Figures 3E–3G). The overall pattern of cytokine induction suggested that Nec-1-s-treated mice had increased levels of proinflammatory cytokines over the DMSO control (Figure 3H; Table S4). RIPK1 inhibition was associated with increased inflammation seen in histological sections and increased adiposity (Figure 3I). Thus, inhibition of necroptosis by Nec-1 s treatment or *Mlkl*$^{-/-}$ deletion leads to increased inflammation but impaired staphylococcal killing.

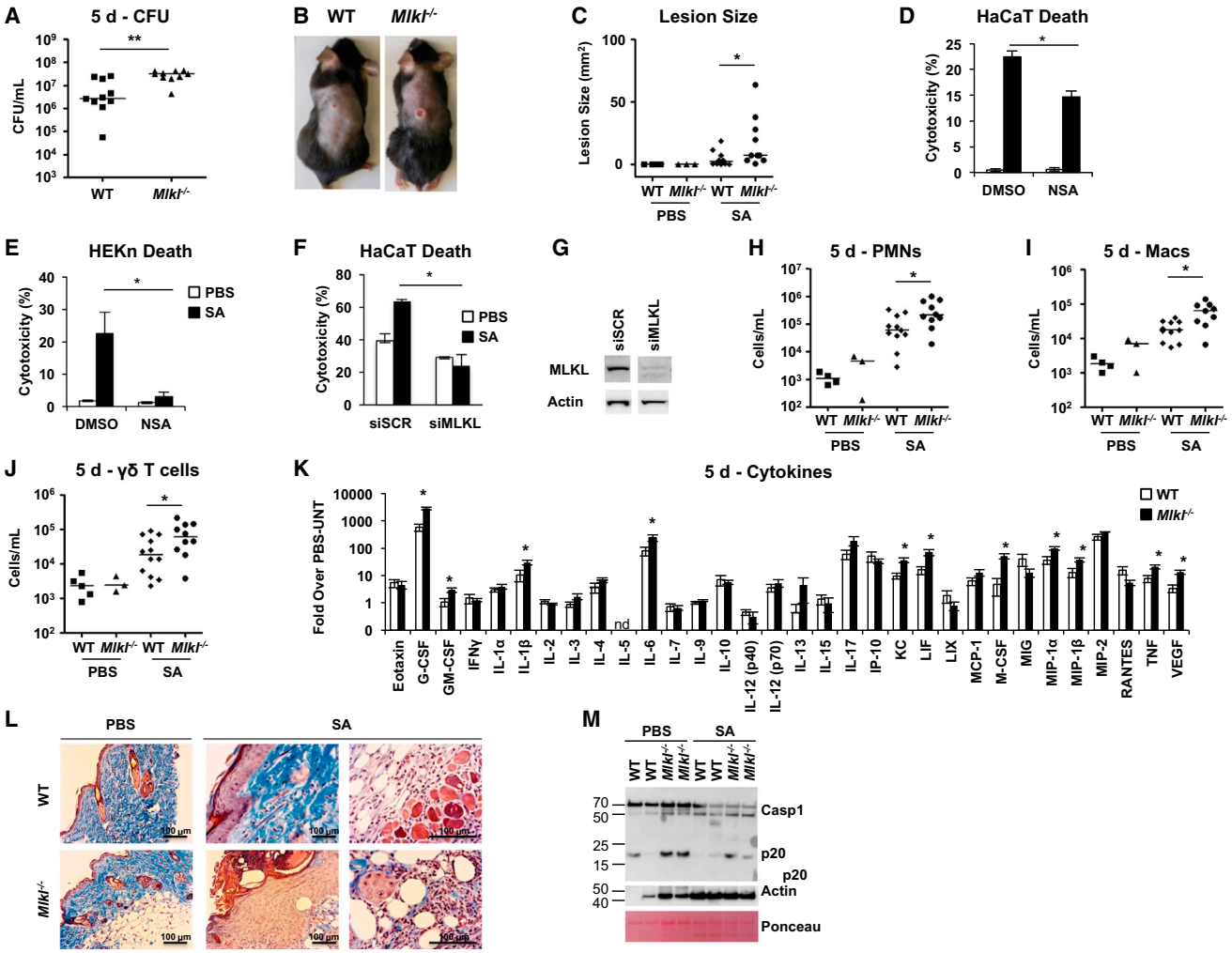

Figure 1. MLKL Contributes to the Clearance of *S. aureus* from Infected Skin

(A–I) *Mlkl*$^{-/-}$ and wild-type (WT) mice were infected subcutaneously with 2 × 10^6 CFUs/mouse of *S. aureus* (SA) for 5 days and the area of infection biopsied for analysis.

(A) *S. aureus* colony forming units (CFUs) recovered.

(B) Representative images of mice showing skin lesions caused by *S. aureus* infection.

(C) Quantification of lesion sizes from (B).

(D and E) Cytotoxicity in HaCaT (C) or primary keratinocytes (HEKn; D) pretreated with 10 μM necrosulfonamide (NSA) and infected with WT *S. aureus*.

(F) Cytotoxicity in *MLKL*-deficient HaCaT infected with *S. aureus* for 4 hr.

(G) Immunoblot of HaCaT with *MLKL* knocked down by siRNA or scrambled control.

(H–J) Number of neutrophils (PMNs) (H), macrophages (Macs) (I), and gamma-delta (γδ) T cells (J) on *Mlkl*$^{-/-}$ and WT mice.

(K) Cytokines from *S. aureus*-infected WT and *Mlkl*$^{-/-}$ mice ("nd" means "not detected").

(L) Representative images of trichrome stain on skin biopsies of PBS or *S. aureus*-infected mice. The scale bars represent 100 μm.

(M) Western blot showing cleaved caspase-1 (p20), full-length caspase-1, actin, and Ponceau on skin homogenate of infected WT and *Mlkl*$^{-/-}$ mice.

Each point represents a mouse, and lines show median values. Data are represented as bar graphs with mean ± SEM. Results shown are pooled from at least two independent experiments. *p < 0.05; **p < 0.01. See also Figures S1 and S2 and Tables S1 and S2.

Ripk3$^{-/-}$ Mice Have Enhanced *S. aureus* Clearance from the Skin

RIPK3 is a target of RIPK1 and a major effector of necroptosis (Christofferson et al., 2014; Vanden Berghe et al., 2014b). However, in contrast to MLKL, which functions as an effector of necroptosis alone, RIPK3 can directly activate apoptosis and stimulate the NLRP3 inflammasome to generate IL-1β (Newton and Manning, 2016). After documenting that an inhibitor of RIPK3, GSK'872, blocked *S. aureus*-induced cytotoxicity in keratinocytes (Figure 4A), we wanted to understand the role of RIPK3 during *S. aureus* skin infection. Using the model of cutaneous *S. aureus* infection, we noted significantly improved outcomes in the *Ripk3*$^{-/-}$ mice with decreased staphylococcal burden (Figures 4B–4D). Significantly fewer inflammatory cells and decreased cytokine production, including IL-1β and granulocyte colony stimulating factor (G-CSF), were observed

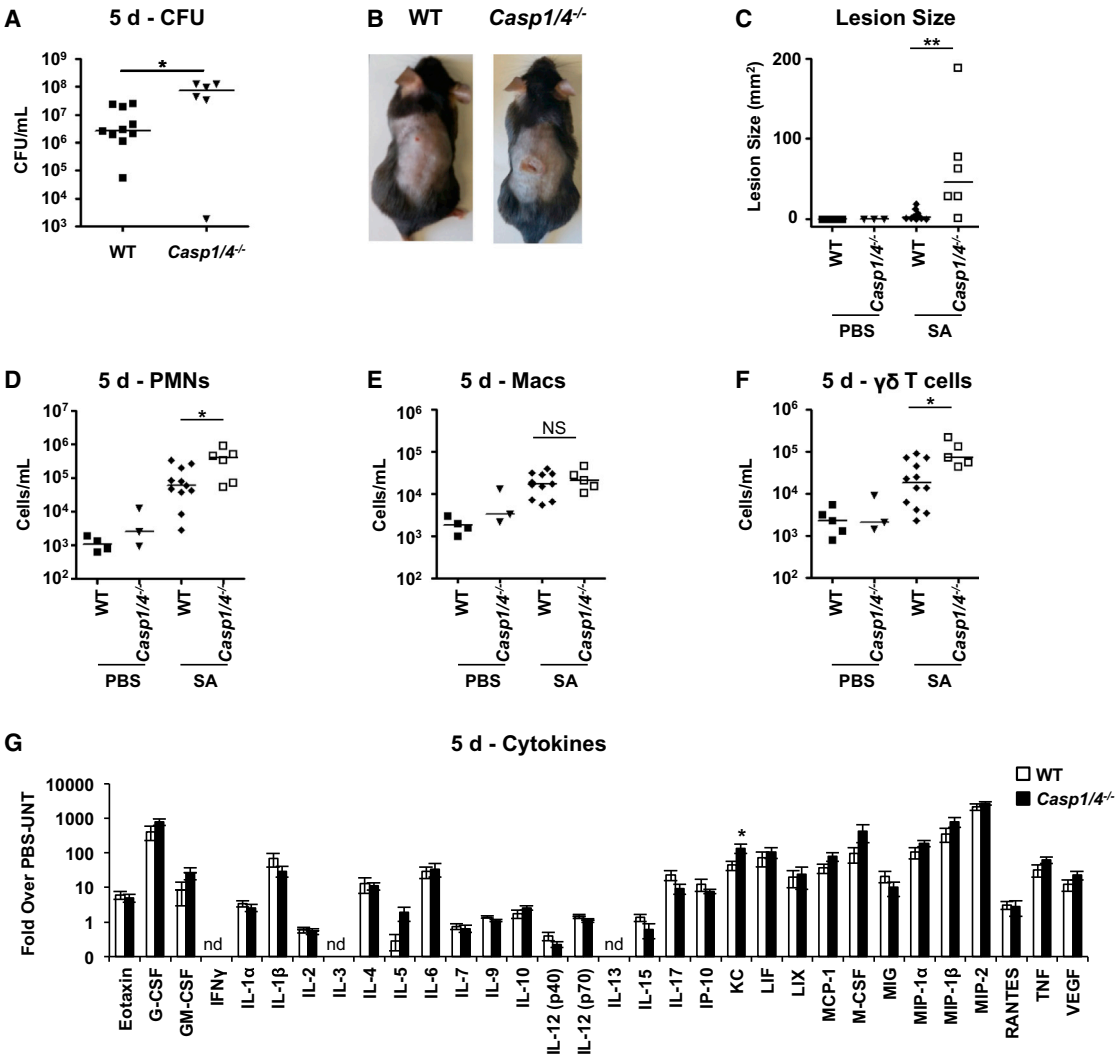

Figure 2. Lack of Caspases-1/4 Is Detrimental in *S. aureus* Skin Infection

Casp1/4$^{-/-}$ and wild-type (WT) mice were infected subcutaneously with 2 × 10^6 CFUs/mouse of SA for 5 days and the area of infection biopsied for analysis.

(A) *S. aureus* CFUs recovered.

(B) Representative images of mice showing skin lesions caused by *S. aureus* infection.

(C) Quantification of lesion sizes from (B).

(D–F) Number of PMNs (D), Macs (E), and γδ T cells (F) on *Mlkl*$^{-/-}$ and WT mice.

(G) Cytokines from *S. aureus*-infected WT and *Mlkl*$^{-/-}$ mice.

Each point represents a mouse, and lines show median values. Data are represented as bar graphs with mean ± SEM. Results shown are pooled from at least two independent experiments. *p < 0.05; **p < 0.01. See also Table S3.

following infection, with similar baseline cytokine activity in *Ripk3*$^{-/-}$ mice compared to WT mice (Figures 4E–4H; Table S5). In contrast to *Mlkl*$^{-/-}$ mice that had *increased* IL-1β production (Figure 1K), the *Ripk3*$^{-/-}$ mice had significantly less IL-1β (Figure 4H). Histopathology was notable for better preservation of skin architecture in the infected *Ripk3*$^{-/-}$ mice (Figure 4I). The interactions of RIPK3 with additional binding partners were evident, as we observed less cell death due to apoptosis, as shown by decreased annexin V staining in both keratinocytes and immune cells in *Ripk3*$^{-/-}$ skin after infection (Figure 4J). Thus, deletion of *Ripk3* inhibited excessive inflammatory signaling and enhanced eradication of *S. aureus* from infected skin.

Caspases-8, -3, and -7 Are Activated by *S. aureus* but Do Not Contribute to Cytotoxicity

Apoptosis and necroptosis share upstream effectors, with RIPK1-FADD-caspase-8 cascade mediating apoptosis and RIPK1-RIPK3-MLKL pathway regulating necroptosis in the absence of active caspase-8 (Chan et al., 2015). Caspase-8 targets the deubiquitinase CYLD, preventing RIPK1 initiation of necroptosis (Legarda et al., 2016). *S. aureus* has been shown

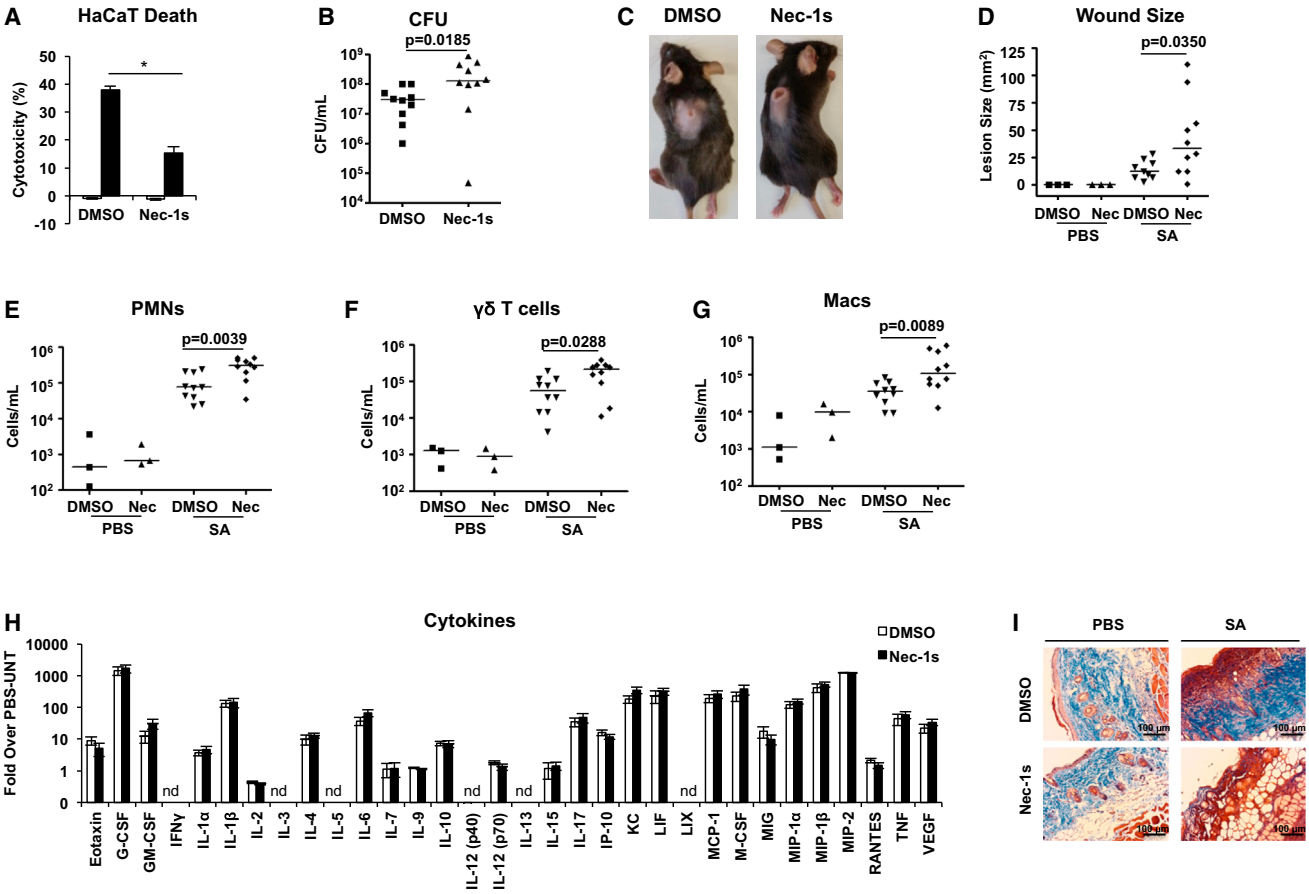

Figure 3. Pharmacological Blockade of Necroptosis Leads to Worse Outcome during *S. aureus* Skin Infection

(A) Cytotoxicity in keratinocyte cell line (HaCaT) pretreated with necrostatin-1 stable (Nec-1 s) and infected with *S. aureus* MOI10 for 4 hr.

(B–I) Mice were infected subcutaneously with SA and treated with 10 mg/kg Nec-1 s or DMSO control for 5 days and their skin tissues biopsied for analysis.

(B) *S. aureus* CFUs recovered on day 5 from Nec-1 s (N) or DMSO-treated mice are shown.

(C) Representative images of mice showing lesions on day 5 of skin infection are shown.

(D) Quantification of lesion sizes on day 5 is shown.

(E–G) Number of PMNs (E), γδ T cells (F), and Macs (G) on infected area is shown.

(H) Cytokines from *S. aureus*-infected mice are shown.

(I) Representative images of trichrome stain on skin biopsies of PBS or *S. aureus*-infected mice are shown. The scale bars represent 100 μm.

Each point represents a mouse, and lines show median values. Data are represented as bar graphs with mean ± SEM. Results shown are pooled from at least two independent experiments. *p < 0.05; **p < 0.01. See also Figure S3 and Table S4.

previously to activate caspases-8, -3, and -7 in keratinocytes (Soong et al., 2012). Because apoptosis and necroptosis effectors are intertwined and because *S. aureus* has the ability to activate both mechanisms of cell death, we wanted to dissect which of the pathways predominate during infection. We observed that *S. aureus* activated caspases-8, -3, and -7 in macrophage and keratinocyte cell lines (Figures 5A–5C). WT as well as toxin-deficient (*agr* mutant) strains of *S. aureus* activated caspases-3/7 to the same extent (Figure 5B). However, deletion of *caspase-8*, as tested in *Casp8*$^{-/-}$*Ripk3*$^{-/-}$ bone-marrow-derived macrophages (BMDMs), did not affect the overall cytotoxicity of *S. aureus* (Figure 5D) because they still express inflammasome components. Similarly, pharmacological inhibitors of the apoptosis executioners (caspases-3/7), which decreased the activation of these caspases (Figure 5C), did not prevent *S. aureus*-induced cytotoxicity in THP-1 cells (Figure 5E). To document the induction of apoptosis in vivo, we demonstrated active caspase-3 in the sloughing corneocyte layer of keratinocytes on *S. aureus*-infected murine skin (Figure 5F). *S. aureus* toxins activate necroptosis (Kitur et al., 2015), as well as pyroptosis (Muñoz-Planillo et al., 2009, 2013; Soong et al., 2012). Thus, whereas *S. aureus* can induce apoptosis executioners, nonetheless, cytotoxicity is mediated predominantly by the components of the inflammasome and the RIPK1/RIPK3/MLKL necroptosis pathways.

Caspase-1 Signaling, but Not Necroptosis, Contributes to *S. aureus* Killing

In vitro assays were performed to establish whether necroptosis participates in *S. aureus* killing by human keratinocytes or

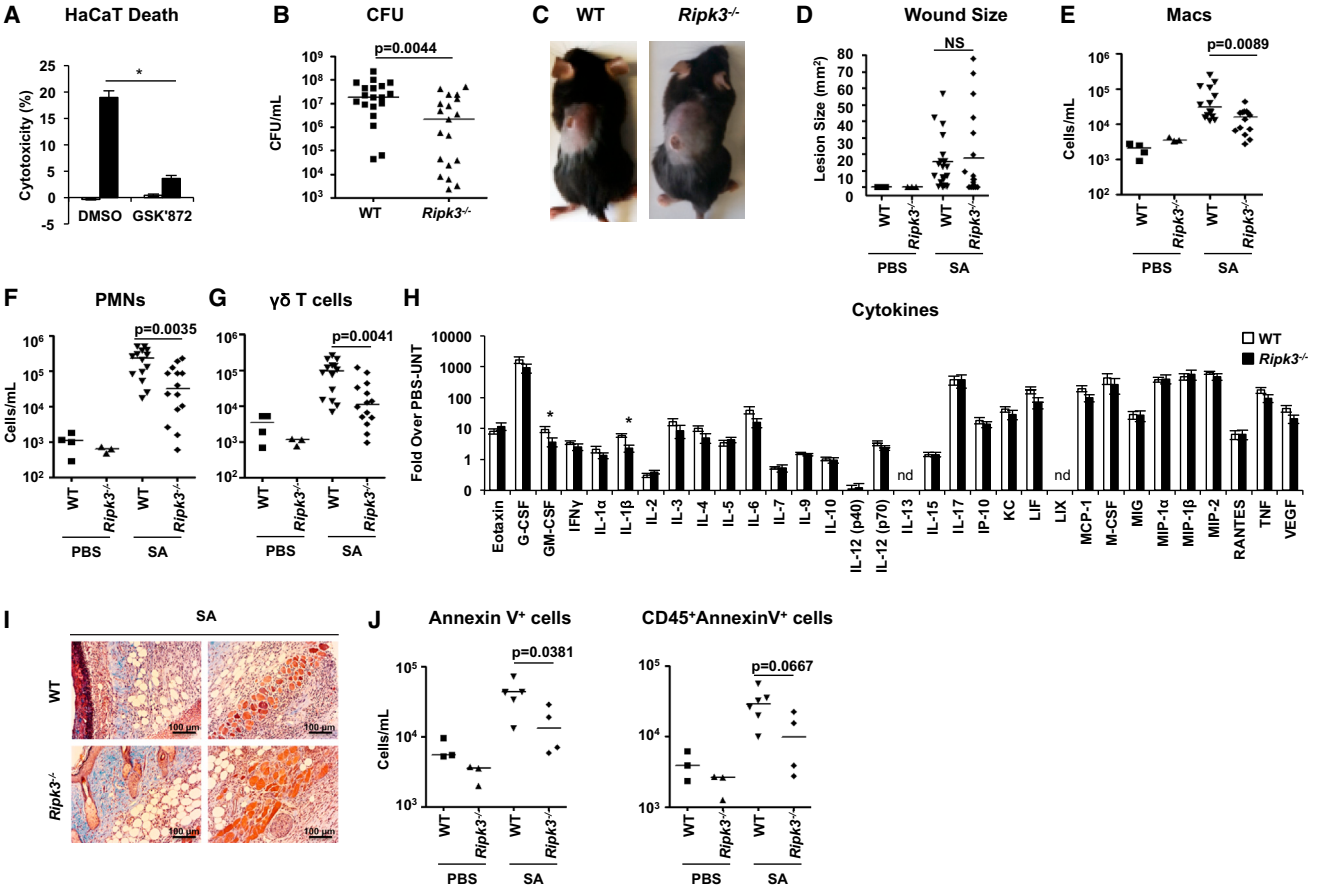

Figure 4. *Ripk3*$^{-/-}$ Mice Have Improved Outcome in *S. aureus* Skin Infection

(A) Cytotoxicity in HaCaT pretreated with 10 μM GSK'872 and infected with *S. aureus*.

(B–J) *Ripk3*$^{-/-}$ and WT mice were infected subcutaneously with SA for 5 days and skin tissues biopsied for analysis.

(B) *S. aureus* CFUs recovered on day 5 on day of infection are shown.

(C) Representative images of mice showing lesions on day 5 of skin infection are shown.

(D) Quantification of lesion sizes on day 5 is shown.

(E–G) Number of PMNs (E), γδ T cells (F), and Macs (G) on infected area is shown.

(H) Cytokines after 5 days of infection are shown.

(I) Representative images of trichrome stain on skin biopsies of *S. aureus*-infected mice are shown. The scale bars represent 100 μm.

(J) Number of total annexin V$^+$ cells and number of annexin V$^+$ immune cells (CD54$^+$) after 5 days of infection are shown.

Each point represents a mouse, and lines show median values. Data are represented as bar graphs with mean ± SEM. Results shown are pooled from at least two independent experiments. *p < 0.05; **p < 0.01. See also Table S5.

immune cells. A gentamicin protection assay performed using human keratinocytes in primary culture demonstrated that concentrations of NSA that prevent cytotoxicity fail to inhibit *S. aureus* killing in contrast to the pan-caspase inhibitor, ZVAD (Figures 1E and 6A). Peritoneal exudate cells (PECs) from the *Ripk3*$^{-/-}$ and *Mlkl*$^{-/-}$ mice had no defect in their ability to phagocytose and kill *S. aureus*, whereas the *Casp1/4*$^{-/-}$ PECs had significantly impaired bacterial killing ability (Figures 6B and 6C). These results were confirmed with BMDMs, demonstrating a lack of effect of the *Ripk3* or *Mlkl* mutation on either staphylococcal killing or the generation of IL-1β, in contrast to the significant contribution of caspase-1 in these processes (Figures 6D–6F). Lack of caspase-1 did not completely abrogate the generation of IL-1β, suggesting that multiple pathways are involved in the production of this cytokine (Figure 6F). To determine the contribution of apoptosis to bacterial killing, we incubated BMDMs from *Casp8*$^{-/-}$*Ripk3*$^{-/-}$ mice with *S. aureus*. *Casp8*$^{-/-}$*Ripk3*$^{-/-}$ BMDMs had no defect in either bacterial uptake or killing abilities (Figures 6G and 6H). *Casp8*$^{-/-}$*Ripk3*$^{-/-}$ BMDMs produce more IL-1β compared to WT BMDMs (Figure 6I), potentially because the lack of both necroptosis and apoptosis components is compensated by the upregulation of the inflammasome products. Thus, caspase-1-mediated responses, but not necroptosis or apoptosis, contribute to staphylococcal death within immune cells and keratinocytes.

MLKL and Caspase-1 Enhance Survival in a Murine Model of *S. aureus* Sepsis

Our results using the skin model of infection reflect participation of RIPK1 and MLKL in staphylococcal clearance by limiting local

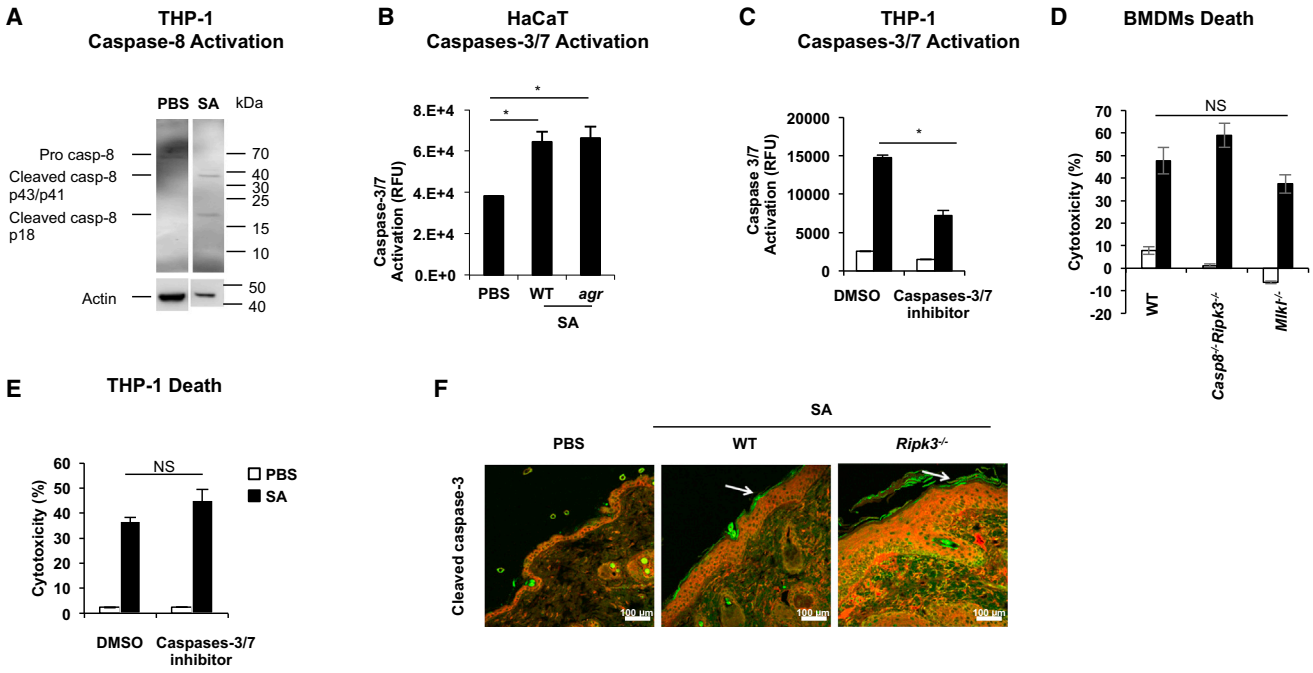

Figure 5. Activation of Caspases-8, -3, and -7 by *S. aureus*

(A) Western blot showing caspase-8 activation in THP-1 cells after *S. aureus* infection.

(B) Caspases-3/7 activation in HaCaT cells pretreated with 20 μM caspase-3/7 inhibitor or DMSO for 1 hr and stimulated with WT or *agr S. aureus* strains for 4 hr.

(C) Caspases-3/7 activation in THP-1 cells pretreated with 20 μM caspase-3/7 inhibitor or DMSO for 1 hr and stimulated with *S. aureus* for 2 hr.

(D) Cytotoxicity in WT, *Casp8*$^{-/-}$*Ripk3*$^{-/-}$, and *Mlkl*$^{-/-}$ BMDMs after *S. aureus* infection.

(E) Cytotoxicity in THP-1 cells treated with DMSO or caspases-3/7 inhibitor and infected with *S. aureus* for 2 hr.

(F) Confocal images of skin biopsies obtained from *S. aureus*-infected WT and *Ripk3*$^{-/-}$ mice and stained for pan cytokeratin (red) and cleaved caspase-3 (green, arrow). Magnification of 200×; scale bars, 100 μm.

Each point represents a mouse, and lines show median values. Data are represented as bar graphs with mean ± SEM. Results shown are pooled from at least two independent experiments. *$p < 0.05$; **$p < 0.01$.

inflammation. As systemic inflammation is a major factor in the morbidity associated with *S. aureus* infections, we used a murine model of bacteremia to compare bacterial clearance when necroptosis is inhibited with Nec-1 s and to highlight the participation of immune cells. Significantly greater numbers of *S. aureus* were recovered from the blood 24 hr after infection in the Nec-1-s-treated mice than from controls (Figure 7A). To confirm the results obtained with Nec-1 s, we used GSK3002963, a potent and specific inhibitor of RIP1 kinase activity (Berger et al., 2015), in our mouse model of sepsis. Like Nec-1-s-treated mice, GSK3002963-treated mice had a decreased ability to clear *S. aureus* in the blood compared to mice treated with a vehicle control (Figure 7B). Mortality studies were then performed using the *Mlkl*$^{-/-}$, *Ripk3*$^{-/-}$, and *Casp1/4*$^{-/-}$ mice in a model of sepsis. We predicted that the *Mlkl*$^{-/-}$ mice, which are unable to activate necroptosis as a mechanism to control inflammatory responses, would have worse outcomes and observed their increased mortality (with median survival of 4 days) compared to the WT mice (Figure 7C). Although the *Ripk3*$^{-/-}$ mice are also unable to activate necroptosis, their limited ability to stimulate the inflammasome was predicted to similarly provide protection from excessive inflammation. Survival of the *Ripk3*$^{-/-}$ mice was equivalent to that of the WT mice and significantly improved as compared to *Mlkl*$^{-/-}$ mutants (Figure 7C). *Casp1/4*$^{-/-}$ mice, which have a staphylococcal killing defect as well as deficient inflammasome activation, had significantly increased mortality (median survival of 2 days; Figure 7C). The outcomes from *S. aureus* sepsis model are consistent with those observed in the skin, in that mutations in the necroptosis pathway associated with excessive inflammatory responses are also associated with negative outcomes.

DISCUSSION

Our findings suggest that necroptosis in the setting of either local or systemic *S. aureus* infection markedly contributes to improved outcome, not by participating in bacterial death but by limiting the damage caused by excessive inflammation. The importance of IL-1 signaling (Miller and Cho, 2011) and the critical role of caspase-1 in *S. aureus* staphylococcal killing (Cohen and Prince, 2013; Sokolovska et al., 2013) are well established. The mechanisms in place to regulate the toxic effects of these cytokines are less well understood. In skin and systemic models of infection, lack of caspase-1 resulted in significantly increased staphylococcal survival, greater neutrophil recruitment, and increased local pathology. However, the inability to activate necroptosis and the associated increased caspase-1 activity and IL-1β production were also associated with excessive local pathology and impaired staphylococcal clearance.

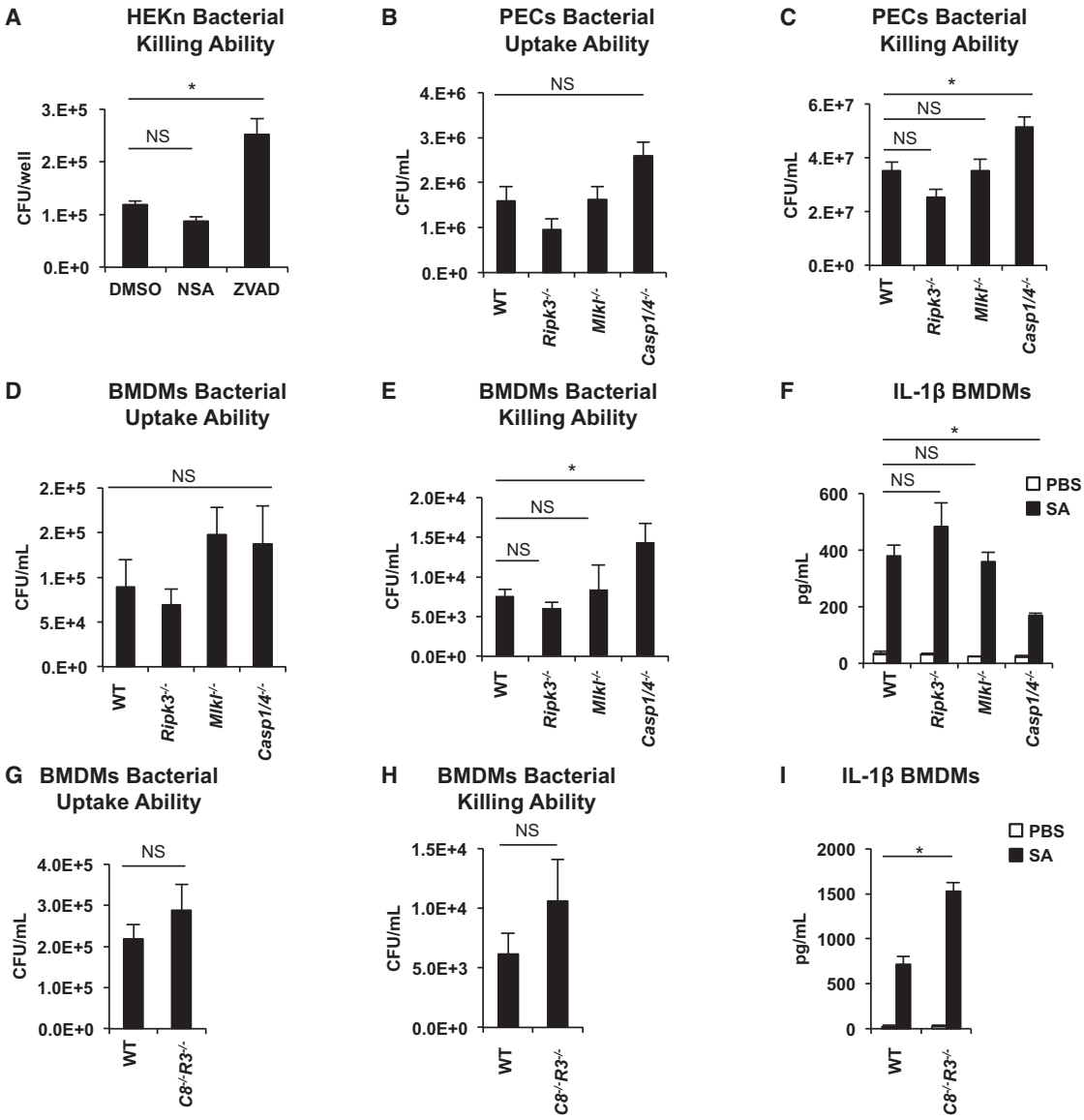

Figure 6. Caspases-1/4 Are Necessary for *S. aureus* Killing by Host Cells

(A) *S. aureus* killing by primary keratinocytes (HEKn cells) pretreated with 10 μM NSA or 50 μM ZVAD, infected with *S. aureus* for 2 hr, and treated with gentamicin for 4 hr.

(B) *S. aureus* uptake by mouse peritoneal exudate cells (PECs) infected with *S. aureus* for 1 hr.

(C) *S. aureus* killing by PECs infected with *S. aureus* for 24 hr.

(D) *S. aureus* uptake by BMDMs from mice after infection for 1 hr.

(E) Gentamicin protection assay showing *S. aureus* killing by BMDMs from WT, *Ripk3*$^{-/-}$, *Mlkl*$^{-/-}$, and *Casp1/4*$^{-/-}$ mice.

(F) IL-1β released by BMDMs from WT, *Ripk3*$^{-/-}$, *Mlkl*$^{-/-}$, and *Casp1/4*$^{-/-}$ mice after stimulation for 4 hr with *S. aureus*.

(G) *S. aureus* uptake by *Casp8*$^{-/-}$*Ripk3*$^{-/-}$ (*C8*$^{-/-}$*R3*$^{-/-}$) BMDMs from mice after infection for 1 hr.

(H) Gentamicin protection assay showing *S. aureus* killing by BMDMs from WT and *Casp8*$^{-/-}$*Ripk3*$^{-/-}$ mice.

(I) IL-1β released by BMDMs from WT and *Casp8*$^{-/-}$*Ripk3*$^{-/-}$ mice after stimulation for 4 hr with *S. aureus*.

Data are represented as bar graphs with mean ± SEM. Results shown are pooled from at least two independent experiments. *p < 0.05.

Several lines of evidence indicate a major role of necroptosis in regulating inflammation. Germline mutations in RIPK1/3, caspase-8, and FADD that interrupt the normal regulation of cell death pathways lead to excessive skin inflammation (Dannappel et al., 2014), even in the absence of a potent stimulus, such as staphylococci. Both *Mlkl*$^{-/-}$ and Nec-1-s-treated mice demonstrate increased *S. aureus* persistence, despite increased phagocyte recruitment and cytokine production. Moreover, *Mlkl*$^{-/-}$ immune cells had no defect in staphylococcal killing. These findings in the setting of common and clinically important

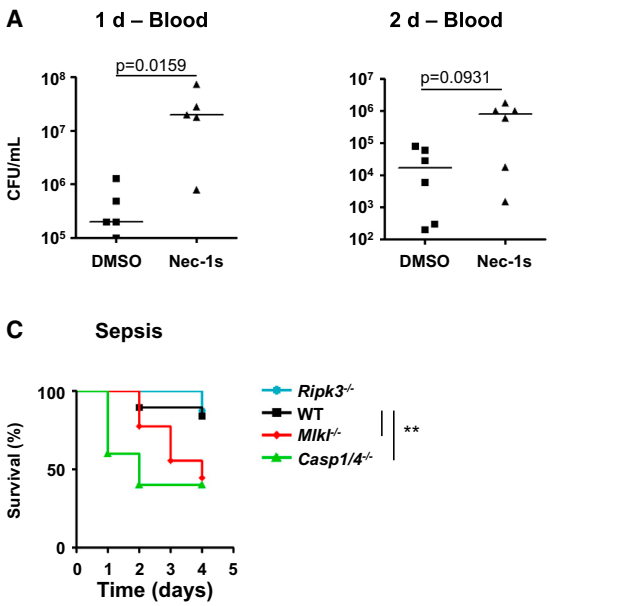

Figure 7. Necroptosis and Caspases-1/4 Are Necessary for Bacterial Clearance and Survival in a Murine Model of *S. aureus* Sepsis

(A) *S. aureus* CFUs recovered from the blood of mice treated with Nec-1 s and infected with 1 × 10^8 CFUs/mouse of *S. aureus* via retro-orbital route. Mice were sacrificed 24 hr or 48 hr after infection.

(B) *S. aureus* CFUs recovered from the blood of mice treated with GSK3002963 and infected with 1 × 10^8 CFUs/mouse of *S. aureus* via retro-orbital route. Mice were sacrificed 24 hr after infection.

(C) Kaplan-Meier survival curves of WT (n = 19), *Ripk3*$^{-/-}$ (n = 8), *Mlkl*$^{-/-}$ (n = 9), and *Casp1/4*$^{-/-}$ (n = 5) mice after retro-orbital injection with 1 × 10^8 CFUs/mouse of *S. aureus*.

Each point represents a mouse, and lines show median values. Results shown are pooled from at least two independent experiments. *p < 0.05; **p < 0.01.

infection are consistent with recent reports indicating that cell death through necroptosis provides a major immune-suppressive function by eliminating the source of cytokine production (Kearney et al., 2015; Stephenson et al., 2016).

Components of the necroptosis cascade are shared among the major cell death pathways and cell fates determined by the nature of the activating stimulus and the local cytokine milieu (Legarda et al., 2016). As we observed, caspase-8 is activated by *S. aureus*, as are the executioner caspases-3/7 as well as RIPK1/RIPK3/MLKL and caspase-1. However, the apoptosis pathway does not participate directly in staphylococcal clearance, nor does it appear to control IL-1β production, as the *Casp8*$^{-/-}$*Ripk3*$^{-/-}$ BMDMs did not have impaired generation of this cytokine, which is critical for *S. aureus* clearance from skin (Abtin et al., 2014; Miller and Cho, 2011; Miller et al., 2006; Nestle et al., 2009). The toxin-mediated cell-death pathways necroptosis and pyroptosis drive cytotoxicity. Our data further document that *S. aureus* activation of caspase-1 and IL-1β production contributes to *S. aureus* killing, as well as to the pathological consequences of inflammation. This is in contrast to the major role of apoptosis in host defense from intracellular pathogens, such as *Yersinia pestis* (Weng et al., 2014), which lack the numerous toxins expressed by *S. aureus* that activate necroptosis (González-Juarbe et al., 2015; Kitur et al., 2015) and inflammasome-mediated pyroptosis (DuMont et al., 2013; Muñoz-Planillo et al., 2009, 2013).

Our data also illustrate the involvement of RIPK3 in multiple cell death and inflammatory responses activated by *S. aureus*. As has been reported by other groups, we observed the effects of RIPK3 (independently of MLKL) in stimulating apoptosis, the NLRP3 inflammasome, and IL-1β production (Lawlor et al., 2015; Newton and Manning, 2016; Pasparakis and Vandenabeele, 2015). The interruption of necroptosis through deletion of *Ripk3* did not reproduce the phenotypes observed in either the *Mlkl*$^{-/-}$ or Nec-1-s-treated mice. Instead, the improved outcome of the *Ripk3*$^{-/-}$ mice in both skin and sepsis models was similar to our previous observations in a model of *S. aureus* pneumonia (Kitur et al., 2015). Lack of *Ripk3* correlated with decreased production of IL-1β and activation of apoptosis, which afforded protection from *S. aureus*-induced inflammatory damage.

The importance of necroptosis in regulating excessive inflammatory signaling was also evident in a model of sepsis. In the absence of *Mlkl*, lethality occurred at a rate significantly greater than in the WT mice, in which the immunoregulatory functions of necroptosis remained intact. Nec-1 s treatment similarly resulted in significantly increased rates of bacteremia early in infection, despite a lack of impairment of *S. aureus* killing by cells unable to undergo necroptosis. The sepsis model also provided the opportunity to observe the importance of caspase-1/4 and its participation in staphylococcal clearance, particularly at the early stages of infection. This was in contrast to the consequences of *Mlkl* deletion that were more apparent over time.

Our findings add to a growing body of literature demonstrating that excessive inflammatory signaling contributes significantly to the morbidity and mortality caused by *S. aureus*, both systemically and at a local site, such as the skin (Kitur et al., 2015; Müller et al., 2015). Our results show that the induction of necroptosis during *S. aureus* infection is an essential component of the host response necessary to limit inflammation. Targeting this pathway or identifying mutations that are associated with its function may provide therapeutic strategies to improve outcome from this common cause of infection.

EXPERIMENTAL PROCEDURES

Bacteria

S. aureus strain MRSA USA300 LAC was grown overnight in Luria broth (LB) at 37°C as previously described (Kitur et al., 2015) and suspended in PBS to achieve the required concentration. *S. aureus* was heat killed at 65°C for 90 min.

Cell Culture

PECs were collected from mice that had been infected intraperitoneally with 10^7 colony-forming units (CFUs) of heat-killed *S. aureus* for 48 hr and 24 hr (Reyes-Robles et al., 2013). *S. aureus* MOI 10 was opsonized for 30 min with 50% normal mouse serum (NMS) (Innovative Research) in RPMI 1640 medium (GIBCO), washed, and suspended in medium. PECs were infected with opsonized *S. aureus* MOI 1 in coated plates for 1 hr and 24 hr. PECs were lysed with 0.1% saponin and recovered bacteria (CFU) enumerated by serial dilutions.

Gentamicin protection assays were performed in HaCaT or BMDMs isolated from mice and differentiated in the presence of 60 ng/ml of mouse M-CSF (Peprotech). After stimulation of HaCaTs for 2 hr or BMDMs for 20 min with *S. aureus* MOI 100, cells were washed and treated with gentamicin (500 μg/ml) for 1 hr or 24 hr. Cells were washed in PBS, lysed with 0.1% saponin, and bacteria enumerated by serial dilution on agar plates.

Cytotoxicity Assays

HaCaT and HEKn cells were grown to confluence in DMEM (GIBCO) and THP-1 cells in RPMI 1640 medium (GIBCO) with 10% fetal bovine serum and 1% penicillin and streptomycin at 37°C and 5% CO_2 in a humidified environment. Cells were maintained in no antibiotic medium 24 hr prior to infection. Cells were pretreated 1 hr prior to infection with Nec-1 s (Enzo Life Technologies), 10 μM necrosulfonamide (NSA) (Calbiochem), 10 μM GSK'872 (Calbiochem), 20 μM caspase-3/7 inhibitor (Promega), or DMSO control (v/v). For siRNA knockdown, HaCaT was grown to confluence and transfected with 100 nM siMLKL (human MLKL siRNA pools of three targets; Santa Cruz Biotechnology) or scrambled siRNA control pool using Lipofectamine RNAiMAX (Life Technologies) as previously described (Kitur et al., 2015). Cells were infected after 3 days of siRNA treatment. *S. aureus* MOI 10 was added to the cells for 4 hr for keratinocytes and 2 hr for macrophages. Lysates were used for immunoblotting and caspases-3/7 activation assays and supernatants for cytotoxicity assays. Lactate dehydrogenase (LDH) cytotoxicity was performed as per manufacturer's instructions (Roche) and as described previously (Kitur et al., 2015). Caspases-3/7 activation was performed as per manufacturer's instructions (Caspase-Glo; Promega).

Model of Skin Infection

Six- to eight-week-old sex-matched WT C57BL/6J (Jackson Laboratory), *Casp1/4*$^{-/-}$ (B6N.129S2-*Casp1*^{tm1Flv}/J; Jackson Laboratory; Kuida et al., 1995), *Ripk3*$^{-/-}$ (Vishva Dixit; Genentech; Newton et al., 2004), and *Mlkl*$^{-/-}$ (John Silke; WEHI via Douglas R. Green; St. Jude Children's Research Hospital; Murphy et al., 2013) were used. Knockouts were backcrossed to C57BL/6J background, and equal sex ratios were used for experiments. Mice were anesthetized, shaved, and inoculated subcutaneously on the back with 2×10^6 CFUs/mouse of *S. aureus* in 100 μl of PBS or with 100 μl PBS (control group) using $26^{5/8}$G sterile needle. Lesions were measured daily, and mice were sacrificed 1 day or 5 days after infection.

Two 3-mm punch biopsy (Premier Uni-Punch) skin specimens were obtained from the lesions of infected mice, and half of the tissue was fixed in 4% paraffin for 1 day and stored in 70% ethanol for histology, performed by the Histology Core at Columbia University Medical Center. Trichrome staining was done, and images were taken on Zeiss Axiocam MRc 5 (Zeiss).

The other half of the specimens was homogenized using a cell strainer to obtain single-cell suspension in 400 μl PBS. Recovered bacteria were enumerated by serial dilutions. Cells were spun down and homogenate used for ELISA and cells stained for fluorescence-activated cell sorting (FACS) as described below.

Model of Sepsis

1×10^8 CFUs of *S. aureus* in 100 μl PBS were delivered intravenously through the retro-orbital injection route to 6- to 8-week-old anesthetized mice and survival monitored daily. For Nec-1 s sepsis experiments, mice were treated with 10 mg/kg Nec-1 s or DMSO control 24 hr prior, during infection, and 4 hr (for 24-hr infection) or 24 hr (for 48-hr infection) after *S. aureus* infection. For GSK3002963 sepsis experiments, mice were treated with 10 mg/kg GSK3002963 reconstituted with 10% DMSO v/v and 20% ethanol v/v in PBS (or reconstitution solution for vehicle control) during infection and 4 hr after *S. aureus* infection. Mice were sacrificed 24 hr or 48 hr after infection and bacteria in blood enumerated and cytokines in blood analyzed as described below.

FACS Analysis

Homogenized cells were prepared as previously detailed (Kitur et al., 2015). Combinations of phycoerythrin (PE) anti-CD54 (YN1/1.7.4; Biolegend), fluorescein isothiocyanate-labeled (FITC) anti-Ly-6G (Gr-1; RB6-8C5; Biolegend), peridinin chlorophyll (PerCP)-Cy5.5-labeled anti-CD11c (N418; Biolegend), allophycocyanin (APC)-labeled anti-MHC II (I-A/I-E; Biolegend), and APC-labeled anti-TCR γδ T cells (γδ T cells) were used. Neutrophils (PMNs) (Ly6G$^+$/MHCII$^-$), macrophages (Macs) (CD11C$^+$/MHCII$^{low\text{-}mid}$), and γδ T cells were enumerated using FlowJo V10.

Cytokine Analysis

Eve Technologies performed Multiplex ELISA on skin homogenate to determine mouse cytokine levels. Only cytokines that induced by infection are shown. IL-1β ELISA immunoblotting was performed as previously described (Kitur et al., 2015).

Immunoblotting and Immunohistochemistry

Cells were lysed using radioimmunoprecipitation (RIPA) buffer as previously described (Kitur et al., 2015). Immuno-detection was done using anti-caspase-1 (p20) (Casper-1; Adipogen), anti-MLKL (Abcam), anti-caspase-8 (Cell Signaling Technology), and β-actin (Sigma-Aldrich) followed by secondary antibodies conjugated to horseradish peroxidase (Santa Cruz Biotechnology). Equal loading was confirmed by staining with 0.1% Ponceau S (w/v) in 5% acetic acid (Sigma-Aldrich).

For immunohistochemistry, sections were stained with cleaved caspase-3 (Cell Signal) and anti-pan cytokeratin (Santa Cruz Biotechnology) followed by peroxidase staining using the Immunocruz ABC Staining kit (Santa Cruz Biotechnology). Control sections were stained with secondary antibodies only.

Ethics Statement

Animal experiments were carried out in strict accordance with the recommendations in the Guide for the Care and Use of Laboratory Animals of the NIH, the Animal Welfare Act, and US federal law. The Institutional Animal Care and Use Committee of Columbia University approved the protocol (AC-AAAH2350 and AC-AAAG7408).

Statistical Analysis

Samples without normal distribution were analyzed using the nonparametric Mann-Whitney test and mouse survival analyzed by log rank (Mantel-Cox) test for comparison of survival curves. Samples with normal distribution were analyzed with two-tailed Student's t test and one-way ANOVA followed by Bonferroni corrections to correct for multiple comparisons. $p < 0.05$ between groups were considered significant. Outliers were determined by Grubb's test and removed. Statistical analysis was performed using GraphPad Prism Version 4.00 (GraphPad). Data are presented as single points with lines representing median values or as bar graphs with mean ± SEM.

For more experimental procedures, see the Supplemental Experimental Procedures.

SUPPLEMENTAL INFORMATION

Supplemental Information includes Supplemental Experimental Procedures, three figures, and five tables and can be found with this article online at http://dx.doi.org/10.1016/j.celrep.2016.07.039.

AUTHOR CONTRIBUTIONS

K.K. and A.P. conceived and designed the experiments. K.K., S.W., A.B., F.P., M.W., G.S., H.F.P., and D.P. performed the experiments. K.K., S.W., A.B., F.P., M.W., G.S., H.F.P., S.B., and D.P. analyzed the data. K.K. and A.P. wrote the paper.

ACKNOWLEDGMENTS

Special thanks to John Silke (WEHI) and Douglas R. Green (St. Jude Children's Research Hospital) for providing us with *Mlkl*$^{-/-}$ mice and Vishva Dixit (Genentech) for *Ripk3*$^{-/-}$ mice. We are grateful to Scott B. Berger and Peter J. Gough (GlaxoSmithKline) for providing us with GSK3002963. We thank John Silke (WEHI), Douglas R. Green (St. Jude Children's Research Hospital), and Razqallah Hakem (UHN, University of Toronto) for providing us with *Casp8*$^{-/-}$*Ripk3*$^{-/-}$ mice bone marrows. Research reported in this publication was performed in the CCTI Flow Cytometry Core, supported in part by the Office of the Director, NIH, under award S10RR027050. The content is solely the responsibility of the authors and does not necessarily represent the official views of the NIH. This work was supported by FONDECYT 1140010, Comisión Nacional de Investigación Científica y Tecnológica, P09-016-F from the Millennium Institute in Immunology and Immunotherapy of the Ministry of Economy of Chile, and Biomedical Research Consortium 13CTI-21526-P5 from INNOVA-CORFO Chile to S.B. and NIH grants 5R01HL079395 and 5R01AI103854 to A.P.

Received: February 26, 2016
Revised: June 9, 2016
Accepted: July 17, 2016
Published: August 11, 2016

REFERENCES

Abtin, A., Jain, R., Mitchell, A.J., Roediger, B., Brzoska, A.J., Tikoo, S., Cheng, Q., Ng, L.G., Cavanagh, L.L., von Andrian, U.H., et al. (2014). Perivascular macrophages mediate neutrophil recruitment during bacterial skin infection. Nat. Immunol. *15*, 45–53.

Aziz, M., Jacob, A., and Wang, P. (2014). Revisiting caspases in sepsis. Cell Death Dis. *5*, e1526.

Berger, S.B., Bertin, J., and Gough, P.J. (2015). Drilling into RIP1 biology: what compounds are in your toolkit? Cell Death Dis. *6*, e1889.

Cai, Z., Jitkaew, S., Zhao, J., Chiang, H.C., Choksi, S., Liu, J., Ward, Y., Wu, L.G., and Liu, Z.G. (2014). Plasma membrane translocation of trimerized MLKL protein is required for TNF-induced necroptosis. Nat. Cell Biol. *16*, 55–65.

Chan, F.K., Luz, N.F., and Moriwaki, K. (2015). Programmed necrosis in the cross talk of cell death and inflammation. Annu. Rev. Immunol. *33*, 79–106.

Christofferson, D.E., Li, Y., and Yuan, J. (2014). Control of life-or-death decisions by RIP1 kinase. Annu. Rev. Physiol. *76*, 129–150.

Cohen, T.S., and Prince, A.S. (2013). Activation of inflammasome signaling mediates pathology of acute P. aeruginosa pneumonia. J. Clin. Invest. *123*, 1630–1637.

Craven, R.R., Gao, X., Allen, I.C., Gris, D., Bubeck Wardenburg, J., McElvania-Tekippe, E., Ting, J.P., and Duncan, J.A. (2009). Staphylococcus aureus alpha-hemolysin activates the NLRP3-inflammasome in human and mouse monocytic cells. PLoS ONE *4*, e7446.

Dannappel, M., Vlantis, K., Kumari, S., Polykratis, A., Kim, C., Wachsmuth, L., Eftychi, C., Lin, J., Corona, T., Hermance, N., et al. (2014). RIPK1 maintains epithelial homeostasis by inhibiting apoptosis and necroptosis. Nature *513*, 90–94.

Degterev, A., Hitomi, J., Germscheid, M., Ch'en, I.L., Korkina, O., Teng, X., Abbott, D., Cuny, G.D., Yuan, C., Wagner, G., et al. (2008). Identification of RIP1 kinase as a specific cellular target of necrostatins. Nat. Chem. Biol. *4*, 313–321.

DuMont, A.L., Yoong, P., Day, C.J., Alonzo, F., 3rd, McDonald, W.H., Jennings, M.P., and Torres, V.J. (2013). Staphylococcus aureus LukAB cytotoxin kills human neutrophils by targeting the CD11b subunit of the integrin Mac-1. Proc. Natl. Acad. Sci. USA *110*, 10794–10799.

Duprez, L., Takahashi, N., Van Hauwermeiren, F., Vandendriessche, B., Goossens, V., Vanden Berghe, T., Declercq, W., Libert, C., Cauwels, A., and Vandenabeele, P. (2011). RIP kinase-dependent necrosis drives lethal systemic inflammatory response syndrome. Immunity *35*, 908–918.

González-Juarbe, N., Gilley, R.P., Hinojosa, C.A., Bradley, K.M., Kamei, A., Gao, G., Dube, P.H., Bergman, M.A., and Orihuela, C.J. (2015). Pore-forming toxins induce macrophage necroptosis during acute bacterial pneumonia. PLoS Pathog. *11*, e1005337.

Kaczmarek, A., Vandenabeele, P., and Krysko, D.V. (2013). Necroptosis: the release of damage-associated molecular patterns and its physiological relevance. Immunity *38*, 209–223.

Kang, T.B., Yang, S.H., Toth, B., Kovalenko, A., and Wallach, D. (2013). Caspase-8 blocks kinase RIPK3-mediated activation of the NLRP3 inflammasome. Immunity *38*, 27–40.

Kang, S., Fernandes-Alnemri, T., Rogers, C., Mayes, L., Wang, Y., Dillon, C., Roback, L., Kaiser, W., Oberst, A., Sagara, J., et al. (2015). Caspase-8 scaffolding function and MLKL regulate NLRP3 inflammasome activation downstream of TLR3. Nat. Commun. *6*, 7515.

Kearney, C.J., Cullen, S.P., Tynan, G.A., Henry, C.M., Clancy, D., Lavelle, E.C., and Martin, S.J. (2015). Necroptosis suppresses inflammation via termination of TNF- or LPS-induced cytokine and chemokine production. Cell Death Differ. *22*, 1313–1327.

Kitur, K., Parker, D., Nieto, P., Ahn, D.S., Cohen, T.S., Chung, S., Wachtel, S., Bueno, S., and Prince, A. (2015). Toxin-induced necroptosis is a major mechanism of Staphylococcus aureus lung damage. PLoS Pathog. *11*, e1004820.

Kuida, K., Lippke, J.A., Ku, G., Harding, M.W., Livingston, D.J., Su, M.S., and Flavell, R.A. (1995). Altered cytokine export and apoptosis in mice deficient in interleukin-1 beta converting enzyme. Science *267*, 2000–2003.

Lawlor, K.E., Khan, N., Mildenhall, A., Gerlic, M., Croker, B.A., D'Cruz, A.A., Hall, C., Kaur Spall, S., Anderton, H., Masters, S.L., et al. (2015). RIPK3 promotes cell death and NLRP3 inflammasome activation in the absence of MLKL. Nat. Commun. *6*, 6282.

Legarda, D., Justus, S.J., Ang, R.L., Rikhi, N., Li, W., Moran, T.M., Zhang, J., Mizoguchi, E., Zelic, M., Kelliher, M.A., et al. (2016). CYLD proteolysis protects macrophages from TNF-mediated auto-necroptosis induced by LPS and licensed by type I IFN. Cell Rep. *15*, 2449–2461.

Linkermann, A., and Green, D.R. (2014). Necroptosis. N. Engl. J. Med. *370*, 455–465.

McLoughlin, R.M., Solinga, R.M., Rich, J., Zaleski, K.J., Cocchiaro, J.L., Risley, A., Tzianabos, A.O., and Lee, J.C. (2006). CD4+ T cells and CXC chemokines modulate the pathogenesis of Staphylococcus aureus wound infections. Proc. Natl. Acad. Sci. USA *103*, 10408–10413.

Miao, E.A., Leaf, I.A., Treuting, P.M., Mao, D.P., Dors, M., Sarkar, A., Warren, S.E., Wewers, M.D., and Aderem, A. (2010). Caspase-1-induced pyroptosis is an innate immune effector mechanism against intracellular bacteria. Nat. Immunol. *11*, 1136–1142.

Miller, L.S., and Cho, J.S. (2011). Immunity against Staphylococcus aureus cutaneous infections. Nat. Rev. Immunol. *11*, 505–518.

Miller, L.S., O'Connell, R.M., Gutierrez, M.A., Pietras, E.M., Shahangian, A., Gross, C.E., Thirumala, A., Cheung, A.L., Cheng, G., and Modlin, R.L. (2006). MyD88 mediates neutrophil recruitment initiated by IL-1R but not TLR2 activation in immunity against Staphylococcus aureus. Immunity *24*, 79–91.

Moriwaki, K., Bertin, J., Gough, P.J., and Chan, F.K. (2015). A RIPK3-caspase 8 complex mediates atypical pro-IL-1β processing. J. Immunol. *194*, 1938–1944.

Müller, S., Wolf, A.J., Iliev, I.D., Berg, B.L., Underhill, D.M., and Liu, G.Y. (2015). Poorly cross-linked peptidoglycan in MRSA due to mecA induction activates the inflammasome and exacerbates immunopathology. Cell Host Microbe *18*, 604–612.

Muñoz-Planillo, R., Franchi, L., Miller, L.S., and Núñez, G. (2009). A critical role for hemolysins and bacterial lipoproteins in Staphylococcus aureus-induced activation of the Nlrp3 inflammasome. J. Immunol. *183*, 3942–3948.

Muñoz-Planillo, R., Kuffa, P., Martínez-Colón, G., Smith, B.L., Rajendiran, T.M., and Núñez, G. (2013). K^+ efflux is the common trigger of NLRP3 inflammasome activation by bacterial toxins and particulate matter. Immunity *38*, 1142–1153.

Murphy, J.M., Czabotar, P.E., Hildebrand, J.M., Lucet, I.S., Zhang, J.G., Alvarez-Diaz, S., Lewis, R., Lalaoui, N., Metcalf, D., Webb, A.I., et al. (2013). The pseudokinase MLKL mediates necroptosis via a molecular switch mechanism. Immunity *39*, 443–453.

Nestle, F.O., Di Meglio, P., Qin, J.Z., and Nickoloff, B.J. (2009). Skin immune sentinels in health and disease. Nat. Rev. Immunol. *9*, 679–691.

Newton, K., and Manning, G. (2016). Necroptosis and Inflammation. Annu. Rev. Biochem. *85*, 743–763.

Newton, K., Sun, X., and Dixit, V.M. (2004). Kinase RIP3 is dispensable for normal NF-kappa Bs, signaling by the B-cell and T-cell receptors, tumor necrosis factor receptor 1, and Toll-like receptors 2 and 4. Mol. Cell. Biol. *24*, 1464–1469.

Pasparakis, M., and Vandenabeele, P. (2015). Necroptosis and its role in inflammation. Nature *517*, 311–320.

Powers, M.E., Becker, R.E., Sailer, A., Turner, J.R., and Bubeck Wardenburg, J. (2015). Synergistic action of Staphylococcus aureus α-toxin on platelets and myeloid lineage cells contributes to lethal sepsis. Cell Host Microbe *17*, 775–787.

Rajala, M.W., and Scherer, P.E. (2003). Minireview: The adipocyte–at the crossroads of energy homeostasis, inflammation, and atherosclerosis. Endocrinology *144*, 3765–3773.

Reyes-Robles, T., Alonzo, F., 3rd, Kozhaya, L., Lacy, D.B., Unutmaz, D., and Torres, V.J. (2013). Staphylococcus aureus leukotoxin ED targets the chemokine receptors CXCR1 and CXCR2 to kill leukocytes and promote infection. Cell Host Microbe *14*, 453–459.

Schäffler, A., and Schölmerich, J. (2010). Innate immunity and adipose tissue biology. Trends Immunol. *31*, 228–235.

Sokolovska, A., Becker, C.E., Ip, W.K., Rathinam, V.A., Brudner, M., Paquette, N., Tanne, A., Vanaja, S.K., Moore, K.J., Fitzgerald, K.A., et al. (2013). Activation of caspase-1 by the NLRP3 inflammasome regulates the NADPH oxidase NOX2 to control phagosome function. Nat. Immunol. *14*, 543–553.

Soong, G., Chun, J., Parker, D., and Prince, A. (2012). Staphylococcus aureus activation of caspase 1/calpain signaling mediates invasion through human keratinocytes. J. Infect. Dis. *205*, 1571–1579.

Soong, G., Paulino, F., Wachtel, S., Parker, D., Wickersham, M., Zhang, D., Brown, A., Lauren, C., Dowd, M., West, E., et al. (2015). Methicillin-resistant Staphylococcus aureus adaptation to human keratinocytes. MBio *6*, pii: e00289-15.

Stephenson, H.N., Herzig, A., and Zychlinsky, A. (2016). Beyond the grave: When is cell death critical for immunity to infection? Curr. Opin. Immunol. *38*, 59–66.

Sun, L., Wang, H., Wang, Z., He, S., Chen, S., Liao, D., Wang, L., Yan, J., Liu, W., Lei, X., and Wang, X. (2012). Mixed lineage kinase domain-like protein mediates necrosis signaling downstream of RIP3 kinase. Cell *148*, 213–227.

Takahashi, N., Duprez, L., Grootjans, S., Cauwels, A., Nerinckx, W., DuHadaway, J.B., Goossens, V., Roelandt, R., Van Hauwermeiren, F., Libert, C., et al. (2012). Necrostatin-1 analogues: critical issues on the specificity, activity and in vivo use in experimental disease models. Cell Death Dis. *3*, e437.

Vanden Berghe, T., Demon, D., Bogaert, P., Vandendriessche, B., Goethals, A., Depuydt, B., Vuylsteke, M., Roelandt, R., Van Wonterghem, E., Vandenbroecke, J., et al. (2014a). Simultaneous targeting of IL-1 and IL-18 is required for protection against inflammatory and septic shock. Am. J. Respir. Crit. Care Med. *189*, 282–291.

Vanden Berghe, T., Linkermann, A., Jouan-Lanhouet, S., Walczak, H., and Vandenabeele, P. (2014b). Regulated necrosis: the expanding network of non-apoptotic cell death pathways. Nat. Rev. Mol. Cell Biol. *15*, 135–147.

Weng, D., Marty-Roix, R., Ganesan, S., Proulx, M.K., Vladimer, G.I., Kaiser, W.J., Mocarski, E.S., Pouliot, K., Chan, F.K., Kelliher, M.A., et al. (2014). Caspase-8 and RIP kinases regulate bacteria-induced innate immune responses and cell death. Proc. Natl. Acad. Sci. USA *111*, 7391–7396.